Am J Cancer Res 2025;15(3):1248-1263
www.ajcr.us /ISSN:2156-6976/ajcr0161551

Original Article

Tissue inhibitor of metalloproteinase 1 as a biomarker of venous invasion in pancreatic ductal adenocarcinoma

You-Na Sung[1,2*], Mi-Ju Kim[3*], Sun-Young Jun[4], Yeon Wook Kim[3], Jihyun Park[5], Sung-Wuk Jang[6], Tae Jun Song[7], Ki Byung Song[8], Seung-Mo Hong[9]

[1]Department of Pathology, Asan Medical Center, University of Ulsan College of Medicine, Seoul, Republic of Korea; [2]Department of Pathology, Korea University Anam Hospital, Korea University College of Medicine, Seoul, Republic of Korea; [3]Biomedical Research Center, Asan Institute for Life Sciences, Asan Medical Center, Seoul, Republic of Korea; [4]Department of Pathology, Incheon St. Mary's Hospital, College of Medicine, The Catholic University of Korea, Seoul, Republic of Korea; [5]Department of Medical Science, Brain Korea 21 Project, Asan Medical Institute of Convergence Science and Technology, Asan Medical Center, University of Ulsan College of Medicine, Seoul, Republic of Korea; [6]Department of Biochemistry and Molecular Biology, University of Ulsan College of Medicine, Seoul, Republic of Korea; [7]Department of Gastroenterology, Asan Medical Center, University of Ulsan College of Medicine, Seoul, Republic of Korea; [8]Department of Surgery, Asan Medical Center, University of Ulsan College of Medicine, Seoul, Republic of Korea; [9]Department of Pathology, Brain Korea 21 Project, Asan Medical Center, University of Ulsan College of Medicine, Seoul, Republic of Korea. [*]Equal contributors.

Received October 29, 2024; Accepted March 12, 2025; Epub March 15, 2025; Published March 30, 2025

Abstract: Pancreatic ductal adenocarcinoma (PDAC) is a fatal disease with a poor prognosis. While venous invasion is believed to contribute to liver metastasis and an unfavorable prognosis, the precise mechanisms involved remain unclear. Here, we conducted gene expression profiling on eight PDAC tissue samples exhibiting portal venous invasion (VI group) compared to PDAC samples without portal venous invasion (CA group) and normal portal vein tissues (NV group). A subset of genes, including tissue inhibitor of metalloproteinase 1 (*TIMP1*), C-X-C motif chemokine receptor 4 (*CXCR4*), olfactomedin-like 2B (*OLFML2B*), and cytochrome P450 family 1 subfamily B member 1 (*CYP1B1*), was found to be specifically expressed in the PDAC group with venous invasion. Immunohistochemical staining of 15 cases revealed significantly higher levels of *TIMP1* (P=.026) and *CXCR4* (P<.001) in the VI set compared to the CA set. In addition, the PDAC group with strong TIMP1 expression had a higher frequency of lymphovascular invasion (P<.001) and lower 5-year survival rates than the PDAC group with no/weak *TIMP1* expression (P=.027). Specific *TIMP1* expression in the venous invasion foci was highlighted on 3D reconstruction imaging. Invasion assays and/or Western blot analyses were performed on pancreatic cancer cells (Panc1), cancer-associated fibroblasts (CAFs), and human endothelial cells (EA.hy926). TIMP1 inhibition suppressed cancer cell invasion in the presence of CAFs. TIMP1 expression increased with PI3Kp110, phospho-AKT, and phospho-ERK1/2 in Panc1 cells co-cultured with CAFs and EA.hy926 endothelial cells. Our data demonstrate that TIMP1 in pancreatic cancer cells promotes venous invasion of PDACs by activating the PI3K/AKT and ERK1/2 pathways in collaboration with CAFs and endothelial cells. Therefore, TIMP1 may serve as a biomarker for venous invasion in PDACs.

Keywords: Pancreas, cancer, vein, invasion, TIMP1, biomarker

Introduction

Pancreatic ductal adenocarcinoma (PDAC) is a fatal disease in the United States and Korea, with a low 5-year overall survival rate [1-3]. Prognostic factors for PDACs include venous and perineural invasions, lymph node metastasis, and positive resection margins [4-9]. Large venous invasion, which involves the portal vein (PV) or superior mesenteric vein (SMV), is frequently observed in PDACs due to the anatomical proximity of the pancreas to these veins. This phenomenon leads to rapid hepatic metastasis, resulting in a poor prognosis for patients with PDACs [10-13]. In addition to venous invasion, the tumor microenvironment is increasingly recognized as a critical determinant of PDAC progression and adverse outcomes [14-16].

The tumor microenvironment of PDAC is composed of various elements, including cancer-

https://doi.org/10.62347/OVUJ4436

associated fibroblasts (CAFs), immune cells, endothelial cells, and the extracellular matrix (ECM), which dynamically interact with tumor cells. These interactions modulate signaling pathways, promoting cancer cell infiltration into adjacent tissues and vessels, and contributing to the complexity of venous invasion. Therefore, understanding the precise mechanisms underlying the muscular venous invasion within the context of the tumor microenvironment is crucial.

Histologic studies have reported that cancer cell clusters often retain epithelial markers like E-cadherin at the point of penetration and destruction of the muscular layer of large veins, suggesting that epithelial-mesenchymal transition (EMT) is not sustained during intravasation [17]. However, the detailed mechanisms underlying venous invasion remain poorly understood. Several studies have investigated gene expression patterns associated with vascular invasion in cancers from different organs, including the liver and uterus [18-21]. Previous studies, including analyses of data from the Cancer Genome Atlas Program (TCGA) [18, 19, 21, 22], primarily compared the genetic mutations or expression levels of PDAC tissues with and without vascular invasion as reported in pathology reports. However, these studies did not compare the tissues based on specific foci with or without venous invasion in PDAC.

Therefore, this study aims to identify candidate genes involved in venous invasion foci using micro-dissected PDAC tissues and gene expression arrays. Furthermore, functional analysis was conducted in conjunction with protein expression validation of the candidate genes.

Materials and methods

Case selection

After receiving approval from the Institutional Review Board (approval number: 2020-0234) with a waiver of informed consent, we collected 23 PDAC cases with PV or SMV invasion and 205 PDACs without PV/SMV invasion from the pathology database.

Tissue preparation and gene expression array

Eight formalin-fixed, paraffin-embedded (FFPE) PDAC tissues with PV or SMV invasion were collected through meticulous manual microdissection and subsequently stained with H&E (Supplementary Figure 1). Each case was categorized into three groups: VI, PDAC with PV/SMV invasion; CA, PDAC in stroma without PV/SMV invasion, representing the PDAC tissue alone; and NV, normal PV/SMV located in close proximity to non-neoplastic pancreatic tissue. RNA was extracted using the FFPE RNeasy kit (Qiagen, Hilden, Germany), and RNA quality was measured with the Agilent BioAnalyzer 2100 (Agilent Technologies, Santa Clara, CA) following the manufacturer's protocol. Twenty-four RNA samples (matched at 8 VI, 8 CA, and 8 NV from each case) were used for gene expression assays using a PanCancer Progression panel (NanoString Technologies, Seattle, WA) with 770 probes containing 730 cancer-related and 40 housekeeping genes. RNA (250-1200 ng) was hybridized with probes, and the RNA transcript number was counted using an nCounter Digital Analyzer (NanoString). Raw data were normalized and analysed using nSolver Analysis software, version 4.0 (NanoString, MAN-C0019-08). The quality of the NanoString data was evaluated using the default parameters specified in the NanoString Gene Expression Data Analysis Guidelines (NanoString, MAN-C0011-04). Background threshold parameters or background subtraction were not selected.

Tissue microarray (TMA)

The validation for protein expression was performed with an independent cohort consisting of 205 PDACs without PV/SMV invasion (CA group) and 15 PDACs containing foci of PV/SMV invasion (VI group). TMAs were constructed from FFPE PDAC tissue blocks using a manual tissue microarrayer (Uni TMA Co. Ltd., Seoul, Republic of Korea). The selection criteria included areas containing >75% of cancer cells without necrosis. TMAs for the CA and VI sets were separately constructed. For the CA set, 2 mm-diameter punches were used to extract four representative PDAC tissue cores from a donor block and transfer them into a recipient block along with one core from matched normal pancreatic tissue. For the VI set, a 4.5 mm-diameter punch was used to transfer a representative core of PV/SMV invasion from a donor block to a recipient block.

Immunohistochemical staining

Immunohistochemical staining was performed on 4 μm-thick sections using a Ventana auto-

stainer with an ultra-View DAB Detection Kit (Ventana, Tucson, AZ), following the manufacturer's instructions. Primary antibodies for tissue inhibitors of metalloproteinase 1 (TIMP1; clone EPR18352, Abcam, Cambridge, UK, 1:500, rabbit monoclonal) and CXCR4 (clone UMB2, Abcam, 1:2000, rabbit monoclonal) were used. For TIMP1, the intensity was assessed based on the highest cytoplasmic intensity observed, utilizing internal controls to ensure objectivity. The scoring criteria were as follows: 0, no staining; 1, weak staining (normal acinar cells); 2, intermediate staining (acinar ductal metaplasia and the muscular layer of arteries); 3, strong staining (pancreatic islets, Supplementary Figure 2). If the area occupied was less than 5%, it was evaluated as 0, regardless of intensity. For CXCR4 immunolabelling, the immunohistochemical score was calculated by multiplying the nuclear intensity (0: no staining; 1: weak staining, contour not visible at 4× but visible at 10×; 2: strong, staining contour distinct at 4×, Supplementary Figure 3) by the fraction (0: 0%; 1: <1/3; 2: 1/3-2/3; 3: >2/3) of expressing tumour cells. If possible, stromal or inflammatory cells should be assessed similarly to tumour cells.

Tissue immunolabelling and 3D imaging

Tissue immunolabelling and 3D imaging after tissue clearing were performed as previously described [17, 23]. In brief, PDAC tissues were incubated and washed with PBS/0.2% Tween-20 and 10 mg/mL heparin. Primary antibodies against cytokeratin 19 (EP1580Y, rabbit monoclonal; 1:200; Abcam), desmin (goat polyclonal; 1:100, LifeSpan Biosciences, Seattle, WA), and TIMP1 (F31P2A5, mouse monoclonal; 1:200; Invitrogen, Waltham, MA) were used. After primary antibody labelling, the tissues were washed, incubated with secondary antibodies, centrifuged, and then sonicated. Then, the tissues were dehydrated with serially concentrated methanol, incubated with dichloromethan, and then transferred to dibenzyl ether overnight for tissue clearing. Immunolabelled tissue structures were viewed in 3D under a confocal laser scanning microscope (LSM800; Carl Zeiss, Jena, Germany). A bandpass filter set with an excitation range of 480/40 nm and an emission range of 525/50 nm was used to visualize the Alexa 488 signals of cytokeratin 19-expressing epithelial cells. A filter set with an excitation range of 400/40 nm and an emission range of 421/50 nm was used to visualize the DyLight 405 signals of desmin-expressing smooth muscle cells. A filter set with an excitation range of 550/40 nm and an emission range of 570/50 nm was used to visualize the Cyanine 3 signals of TIMP1-expressing cells. Then, 3D images were generated with IMARIS software (Version 9.4, Bitplane, Zurich, Switzerland).

Cell culture

The human PDAC cell line Panc1 was provided by Dr. Ji Kon Ryu from Seoul National University Hospital and cultured in Dulbecco's Modified Eagle's Medium (DMEM; Gibco, Waltham, MA). The human endothelial cell line EA.hy926 was obtained from the American Type Culture Collection (ATCC, Manassas, VA) and maintained in DMEM. Human pancreatic cancer-associated fibroblasts (CAFs) isolated from primary PDACs were cultured in RPMI 1640 (Gibco). These cell lines were grown in media supplemented with 10% (v/v) FBS (Wellgene, Gyeongsan, Korea), penicillin (100 U/mL, Gibco), and streptomycin (100 µg/mL, Gibco) at 37°C in a humidified atmosphere with 5% CO_2. Panc1, EA.hy926, and CAFs were indirectly co-cultured to create an environment mimicking venous invasion. Each cell line (1×10^6 cells/dish) in a 60 mm dish was co-cultured with two other cell lines (each 2×10^5 cells/insert) using culture insert (SPL, Pocheon, Korea) with 8.0 µm pore size for indicated times.

siRNA transfection

Human *TIMP1* siRNA was purchased from Ambion (Thermo Fisher Scientific, Waltham, MA). Panc1 cells were transfected with siRNA using Oligofectamine (Invitrogen) according to the manufacturer's protocol. Briefly, Panc1 or CAFs (2×10^5 cells) were transfected with a 0.2 µM siRNA/Oligofectamine complex in media without FBS at 37°C for 4 h and then added FBS to the final 10% concentration. After 48 h, transfected cells were used for invasion assay or Western blot analysis to determine the effect of TIMP1 on the venous invasion of cancer cells. The corresponding target sequences of siRNA are shown as follows: TIMP1, 5'-GAUGUAUAAAGGGUUCCAA-3', and scramble, 5'-UUCUCCGAACGUGUCACGU-3'.

Cancer cell invasion assay

Cancer cell invasion capacity was assessed using the Boyden chamber system with an

Table 1. Clinicopathologic characteristics of PDAC cases

Characteristics		No. of patients (%)
Age, year		63.4 ± 10.6
Sex	Male	130 (57.0%)
	Female	98 (43.0%)
Differentiation	WD	14 (6.1%)
	MD	179 (78.5%)
	PD	35 (15.4%)
Tumour size, cm		3.9 ± 2.0
Lymphovascular invasion	Present	99 (43.4%)
	Absent	129 (56.6%)
Perineural invasion	Present	189 (82.9%)
	Absent	39 (17.1%)
T category	pT1	4 (1.8%)
	pT2	24 (10.5%)
	pT3	200 (87.7%)
N category	pN0	93 (40.8%)
	pN1	104 (45.6%)
	pN2	31 (13.6%)

insert coated with ECM in 24-well plates. The upper chamber, equipped with a pore size of 8.0 μm, was coated with VitroGel hydrogel matrix (TheWell Bioscience, North Brunswick, NJ) at 37°C for 20 min. Subsequently, 1×10^5 EA.hy926 cells were coated in the upper chamber for 6 h, and then CAFs (1×10^5 cells/insert) were incubated overnight in the upper chamber. Panc1 (2×10^5 cells/insert) cells were incubated in the upper chamber with serum-free media, while media containing 10% FBS was added in the lower chamber. A Panc1-free condition was assessed to eliminate the migration effect of EA.hy926 cells, or CAFs (for negative control). After 24 h, the invasive cancer cells successfully infiltrated into the matrix and then adhered to the film at the bottom of the upper chamber. Gentle cotton swabs were applied to the interior of the upper chamber to remove non-invasive cells. Invasive cells were stained using a cell stain solution (Millipore, Darmstadt, Germany) and then dissolved with 10% acetic acid. The invasiveness of cancer cells was assessed using a colorimetric ELISA at a wavelength of 570 nm. All experiments were performed in triplicate.

Western blot analysis

Whole-cell proteins from the cell lines were separated using sodium dodecyl sulfate-polyacrylamide gel electrophoresis (SDS-PAGE) and subsequently transferred to nitrocellulose membranes (Hybond-ECL, GE Healthcare, Chicago, IL). The membranes were incubated with primary antibodies and then with secondary antibodies conjugated with horseradish peroxidase. Enhanced chemiluminescence (Perkin-Elmer, Waltham, MA) was employed to detect specific antigen-antibody complexes. Western blot analysis was performed with the following antibodies: TIMP1 (F31P2A5, Invitrogen), AKT (C67E7, Cell Signaling Technology, Danvers, MA), phospho-AKT (S473, D9E, Cell Signaling Technology), ERK1/2 (137F5, Cell Signal-=ing Technology), phospho-ERK1/2 (Thr202/Tyr204, Cell Signaling Technology), and PI3-Kp110 (C73F8, Cell Signaling Technology), with GAPDH (6C5, Santa Cruz Biotechnology, Dallas, TX) serving as the loading control. Secondary antibodies were obtained from AbClon (Seoul, Korea).

Statistical analysis

Statistical analyses were performed using R software (version 4.0.2, Vienna, Austria). The relationship between each clinicopathologic factor and protein expression was investigated using the chi-squared test or Student's t-test. The quantitative relationship between TIMP1 and CXCR4 expression was compared using the corrgram function in R version 1.14. Statistical significance was defined as $P<.05$.

Results

Clinicopathologic characteristics

The clinicopathologic characteristics of all cases, which included a test set (n=8) and a validation set (n=220), are summarized in **Table 1**. Briefly, the mean age of the patients was 63.4 ± 10.6 years, with a male-to-female ratio of 1.3:1. Moderately differentiated tumours were the most common (179 cases, 78.5%). The mean cancer size was 3.9 ± 2.0 cm. Lymphovascular invasion and perineural invasion were identified in 99 (43.4%) and 189 (82.9%) cases, respectively. Based on the 8th edition of the AJCC cancer staging scheme, pT3 cancers were the most predominant (200 cases, 87.7%).

Candidate genes for venous invasion through the NanoString gene expression assay

Genes with $P<.05$ and an expression difference of more than two-fold between the VI group and

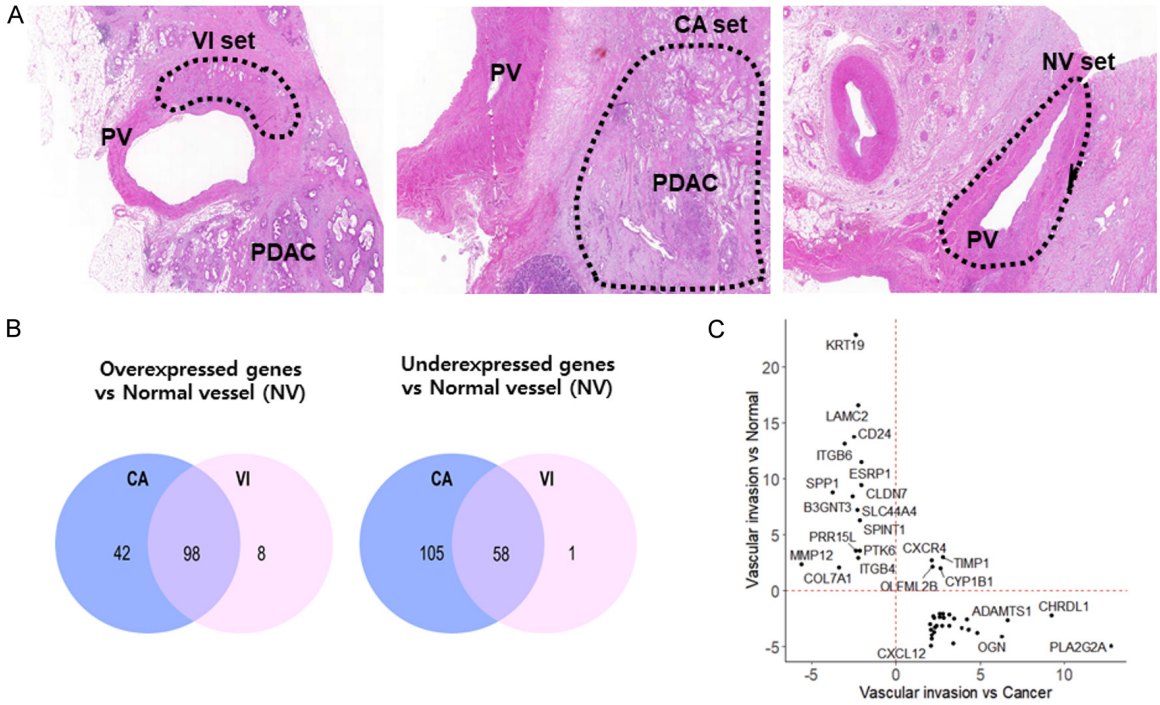

Figure 1. A. Representative H&E staining images of areas before manual microdissection: 1) VI set, portal vein/superior mesenteric vein with cancer cell invasion; 2) CA set, PDAC tissue without portal vein/superior mesenteric vein invasion; and 3) NV set, portal vein/superior mesenteric vein located in close proximity to non-neoplastic pancreatic tissue. Dotted lines indicate the area of microdissection; PV, portal vein; PDAC, pancreatic ductal adenocarcinoma. B. Venn diagrams illustrating candidate genes that are either overexpressed or underexpressed in the VI or CA groups compared to the NV group, with P<0.05 and a difference in expression of more than two-fold. C. Scatter plot showing gene expression fold change in the VI group compared to the CA and NV groups. TIMP1, CXCR4, OLFMI2B, and CYP1B1 were overexpressed in the VI group relative to the CA and NV groups.

the two other groups (CA and NV) were selected for comparison. A total of 165 genes (106 exhibiting overexpression and 59 exhibiting underexpression) in the VI group and 303 genes (140 exhibiting overexpression and 163 exhibiting underexpression) in the CA group were differentially expressed compared to the NV group (**Figure 1A** and **1B**). Among nine specific genes (8 overexpression and 1 underexpression) in the VI group, only four genes (*TIMP1*, *CXCR4*, *OLFMI2B*, and *CYP1B1*) were overexpressed compared with those in the CA and NV groups (**Figure 1C**). Therefore, *TIMP1*, *CXCR4*, *OLFML2B*, and *CYP1B1* were selected as candidate biomarkers for venous invasion.

Protein expression of TIMP1 and CXCR4

Among the four markers (*TIMP1*, *CXCR4*, *OLFML2B*, and *CYP1B1*), the selection of potential biomarkers for venous invasion for protein validation was guided by considerations of biological relevance, the availability of validated antibodies, and supporting evidence from the literature [24-28]. Consequently, TIMP1 and CXCR4 were prioritized for protein validation (**Figure 2**). Based on the intensity of TIMP1 expression, PDACs were categorized into two groups: TIMP1 strong (intensity levels 2 and 3) and TIMP1 weak or absent (intensity levels 0 and 1, **Figure 3A-D**). The rate of strong TIMP1 expression in the VI set was significantly higher (86.7%, 13/15) compared to that in the CA set (53.3%, 90/169, **Figure 3E**, P=.026). Compared with clinicopathologic parameters, the PDAC group with strong TIMP1 expression had more common lymphovascular invasion than that with weak TIMP1 expression (55.6% versus 10.1%, P<.001, **Table 2**). Moreover, the PDAC group with strong TIMP1 expression had a lower 5-year overall survival rate (8.6%) than that with weak/no TIMP1 expression (15.4%, P=.027, **Figure 3F**). The diagnostic performance of TIMP1 for identifying venous invasion was evaluated by calculating sensitivity and specificity using the VI and CA sets. Sensitivity

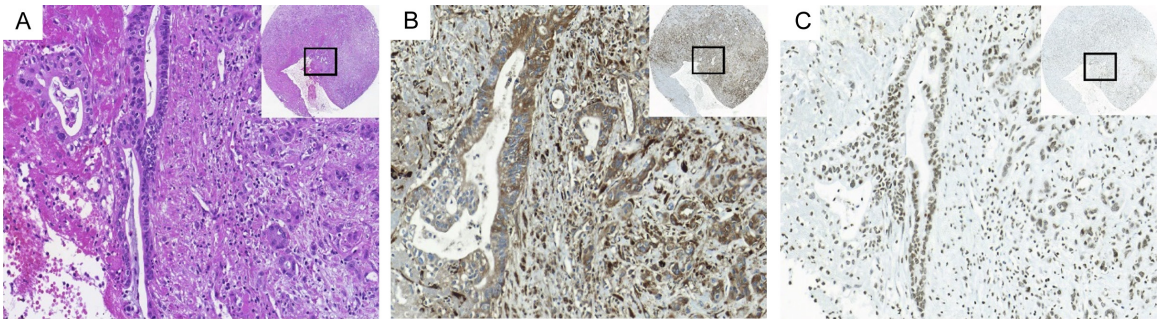

Figure 2. Representative histologic and immunohistochemical staining images of foci of venous invasion. (A) H&E, (B) diffuse strong cytoplasmic TIMP1 immunolabeling in the cytoplasm of cancer cells and CAFs, and (C) diffuse nuclear CXCR4 immunolabeling in the cancer cells and CAFs (all, magnification, 20×; inset, 2.3×).

was defined as the proportion of cases in the VI set exhibiting robust TIMP1 expression, while specificity was defined as the proportion of cases in the CA set lacking robust TIMP1 expression. The sensitivity was 86.7% (13/15), and the specificity was 46.7% (79/169).

The results of CXCR4 immunohistochemical staining were evaluated using immunohistochemical score. Six immunohistochemical scores were generated, with each immunohistochemical score matching the number of instances in the VI/CA set presented in Supplementary Figure 4A. The immunohistochemical score in the VI group (4.73 ± 2.22) for CXCR4 was greater than that in the CA group (1.14 ± 1.48, P <.001, Supplementary Figure 4B). PDACs were divided into two categories based on the immunohistochemical score of CXCR4 expression (strong CXCR4 expression, immunohistochemical score ≥3; weak/no CXCR4 expression, immunohistochemical score <3) and compared with clinicopathologic parameters (Supplementary Table 1). The patients in the PDAC group with strong CXCR4 expression were older than those in the PDAC group with weak/no expression (P=.01). No significant difference in 5-year overall survival was observed between the PDAC groups with strong and weak CXCR4 expression (Supplementary Figure 4C, P=.8, strong CXCR4 expression group; 11.8%, weak/no CXCR4 expression group, 10.6%).

In addition, 3D multi-colour immune-fluorescent labelling images demonstrated TIMP1 expression at the venous invasion foci of the PDAC tissues. Cytoplasmic TIMP1 expression was clearly visible in the tubule-forming cancer cells inside the muscular venous wall and in the CAFs surrounding scattered cancer cells destroying the smooth muscle of the venous wall (**Figure 4**). These results were consistent with the 2D immunohistochemical staining images.

Association between TIMP1 and CXCR4 expression

The expression levels of TIMP1 and CXCR4 in cancer, stromal, and inflammatory cells were compared to analyse the association between TIMP1 and CXCR4 expression. No discernible association was observed between TIMP1 and CXCR4 expression among cancer, stromal, and inflammatory cells, with correlation coefficients of 0.37, 0.35, and -0.01, respectively (Supplementary Figure 5). However, a correlation was noted in the immunohistochemical scores of CXCR4 expression among cancer, stromal, and inflammatory cells (correlation coefficients: cancer-stromal, 0.79; cancer-inflammatory cells, 0.52; stromal-inflammatory cells, 0.53).

TIMP1 expression in the microenvironmental component cells of venous invasion through indirect co-culture

Panc1 cells (cancer cells), EA.hy926 cells (endothelial cells), and CAFs were indirectly co-cultured to mimic the microenvironment of venous invasion and investigate the TIMP1 signaling pathway in each cell type. As the co-incubation time was prolonged, TIMP1 expression was increased in Panc1 cells (**Figure 5A**). Concurrently, the expression of PI3Kp110, as well as phospho-AKT and phospho-ERK1/2, also increased, while the total levels of AKT and ERK1/2 remained unchanged. Under the same conditions, TIMP1 expression was transiently elevated (for 20-40 minutes) in the CAFs.

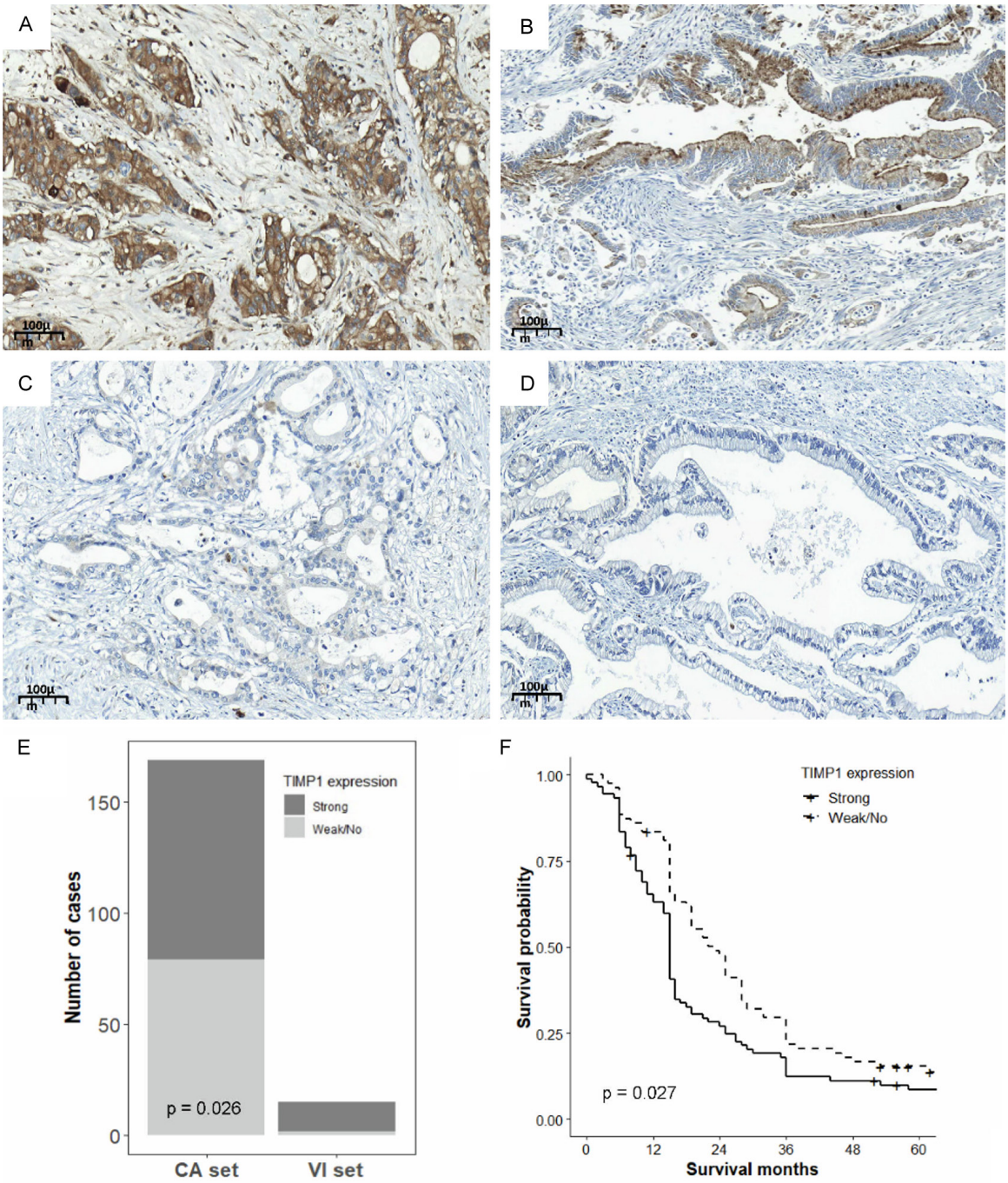

Figure 3. Representative immunohistochemical staining images of TIMP1 in PDAC tissue exhibiting venous invasion. (A) Strong staining (intensity 3). (B) Intermediate staining (intensity 2). (C) Weak staining (intensity 1). (D) No staining (intensity 0; all 20× magnification). TIMP1 intensities of 2 and 3 were classified as strong, while intensities of 1 and 0 were categorized as weak or absent TIMP1 immunolabeling (A-D, 20× magnification). (E) Results of TIMP1 immunolabeling in the VI and CA sets. The proportion of cases exhibiting strong TIMP1 expression in the VI set was 86.7% (13/15), which was significantly higher than in the CA set (53.3%, 90/169; P=.026). (F) The PDAC group with strong TIMP1 expression demonstrated a poorer 5-year overall survival rate of 8.6% compared to 15.4% in the weak/no TIMP1 expression group (P=.027).

PI3Kp110 expression and phospho-AKT increased in the CAFs, but phospho-ERK1/2 levels did not change with co-incubation (**Figure 5B**). In contrast, TIMP1 expression in EA.hy926 cells was minimal and challenging to detect during co-incubation. Nevertheless, the expression of PI3Kp110, along with phospho-AKT and phospho-ERK1/2, increased in EA.hy926 cells

Table 2. Comparison of TIMP1 expression status with clinicopathologic factors of PDACs

Clinicopathologic factor		TIMP1 expression		*P*-value
		Weak/none	Strong	
Age, years		63.3 ± 9.65	62.3 ± 10.5	.55
Sex	Male	47 (59.5%)	46 (51.1%)	.35
	Female	32 (40.5%)	44 (48.9%)	
Differentiation	Well-differentiated	9 (7.6%)	3 (3.3%)	.24
	Moderately differentiated	63 (79.7%)	69 (76.7%)	
	Poorly differentiated	10 (12.7%)	18 (20.0%)	
Tumour size, cm		3.9 ± 2.4	3.9 ± 1.8	.84
Lymphovascular invasion	Present	8 (10.1%)	50 (55.6%)	<.001[a]
	Absent	71 (89.9%)	40 (44.4%)	
Perineural invasion	Present	62 (78.5%)	75 (83.3%)	.54
	Absent	17 (21.5%)	15 (16.7%)	
T category	pT1	2 (2.5%)	1 (1.1%)	.31
	pT2	5 (6.3%)	2 (2.2%)	
	pT3	72 (91.1%)	87 (96.7%)	
N category	pN0	39 (49.4%)	37 (41.1%)	.47
	pN1	35 (44.3%)	44 (48.9%)	
	pN2	5 (6.3%)	9 (10%)	

[a]Statistically significant at P<.05.

as the co-incubation time was prolonged (**Figure 5C**).

Impact of TIMP1 signaling pathways on venous invasion in PDAC cells

In TIMP1 knockdown Panc1 cells, the expression levels of PI3Kp110, phospho-AKT, and phospho-ERK1/2 were significantly reduced, and these levels did not increase following co-culture with CAFs and EA.hy926 cells (**Figure 5D**). The TIMP1 knockdown in Panc1 cells also impaired their invasive ability (1.3-fold decrease, P=.005; **Figure 5E**). Moreover, the invasion capability of Panc1 cells was reduced by targeting the TIMP1 downstream proteins using the PI3K inhibitor LY294002 (10 μM) and the ERK inhibitor PD98059 (50 μM) in the presence of CAFs (both showing a 2.1-fold decrease, P<.001; **Figure 5F**). These results demonstrate that TIMP1 promotes venous invasion through the activation of the PI3K/AKT and ERK1/2 pathways in PDAC cells.

Impact of TIMP1 expression in CAFs on venous invasion of PDAC cells

The invasion capability of Panc1 cells was evaluated with varying quantities of CAFs. The increase in invading Panc1 cells correlated with a higher quantity of CAFs (P<.001; Supplementary Figure 6A), suggesting that CAFs play a significant role in the venous invasion of PDAC cells. Following a transient increase in TIMP1 expression in CAFs, Panc1 cells also exhibited an increase in TIMP1 levels (**Figure 5A** and **5B**). In the absence of CAFs, Panc1 cells failed to induce TIMP1 expression and activate the PI3K/AKT pathway when co-cultured with EA.hy926 cells (Supplementary Figure 6B). The invasion capability was unaffected by TIMP1 knockdown in Panc1 cells (**Figure 5E**) or by the use of a PI3K inhibitor in the absence of CAFs (**Figure 5F**). Although Panc1 cells showed activation of ERK1/2 when co-cultured with EA.hy926 cells (Supplementary Figure 6B), the invasion ability of Panc1 cells was not significantly reduced by ERK1/2 inhibitors (P=.103; **Figure 5F**).

To further investigate the role of TIMP1 in CAFs on the invasion capability of Panc1 cells, TIMP1 knockdown CAFs were utilized. The inhibition of TIMP1 in CAFs reduced the invasion capability of Panc1 cells to levels comparable to those observed in the absence of CAFs (1.4-fold decrease, P=.021; **Figure 5G**). Consequently, these findings indicate that TIMP1 derived from CAFs enhances the venous invasion of PDAC cells through the activation of the TIMP1/PI3K/

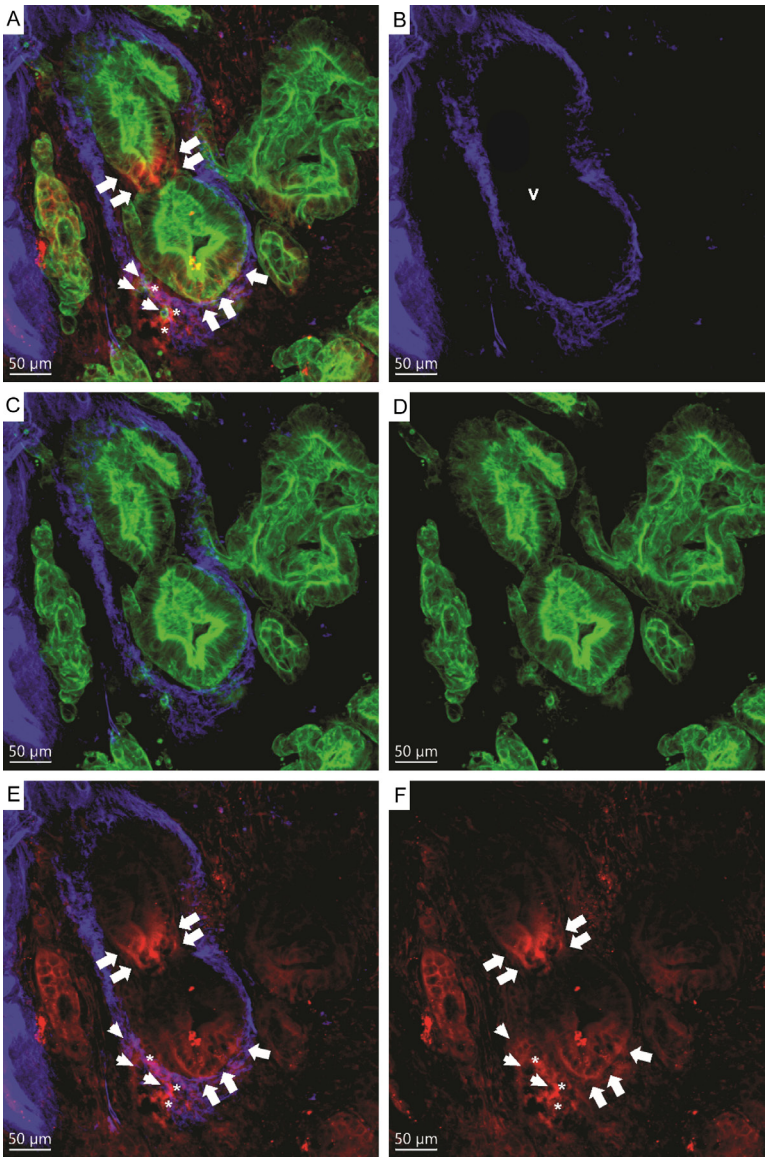

Figure 4. Multi-colour immunofluorescence labelling of 3D reconstruction of PDAC tissue at the foci of venous invasion. Green labelling for cytokeratin 19 highlights cancer cells, red indicates TIMP1 and blue labelling for desmin highlights the muscular layer of the muscular vein. A. Merged cytokeratin 19, desmin, and TIMP1 images. Cytoplasmic TIMP1 expression was clearly visible in tubule-forming cancer cells (arrows) inside the muscular venous wall, and CAFs (asterisks) surrounding scattered cancer cells (arrowhead) destroying the smooth muscle of the venous wall. B. Desmin image. C. Merged cytokeratin 19 and desmin image. D. Cytokeratin image. E. Merged TIMP1 and desmin image. F. TIMP1 image. V, vein.

AKT pathway, facilitated by molecular interactions between CAFs and cancer cells.

Discussion

In this study, we profiled gene expression and identified *TIMP1* as a differentially expressed gene at the foci of venous wall invasion in PDACs. In addition, we found that TIMP1 protein expression was significantly stronger in the PDAC group with venous invasion compared to the group without venous invasion. Patients in the PDAC group exhibiting high TIMP1 expression had a lower overall survival rate than those with no or weak TIMP1 expression. Utilizing publicly available data from sources such as TCGA and Oncomine, the majority of studies have demonstrated a correlation between TIMP1 mRNA expression and an unfavourable prognosis [25, 26, 29, 30]. Moreover, TIMP1 overexpression has been related to poor prognosis in patients with kidney [26], breast [31-33], colon [25, 30, 34], stomach [35-37], lung [38, 39], liver [24], endometrial cancers [40], PDAC [41-43], and malignant melanomas [29, 44]. In addition, the PDAC group with strong TIMP1 expression exhibited a higher frequency of lymphovascular invasion compared to the group with weak TIMP1 expression, suggesting that TIMP1 may play a role in the invasion of large muscular venous walls.

TIMP1 is a pleiotropic extracellular protein that belongs to the TIMP family. It was initially reported to prevent cancer invasion and metastasis by inhibiting the expression of matrix metalloproteinases (MMPs) [45-47]. However, several recent studies have demonstrated that TIMP1 can modulate angiogenesis, EMT, and cell proliferation in a manner distinct from the inhibition of MMPs [47-50]. TIMP1 expression has been linked to tumour budding in breast cancer [51] and metastasis in hepatocellular carcinoma [24, 52, 53], colon cancer [24, 52, 53], and PDAC [54-56]. The secreted TIMP1 from PDAC tissues interacts

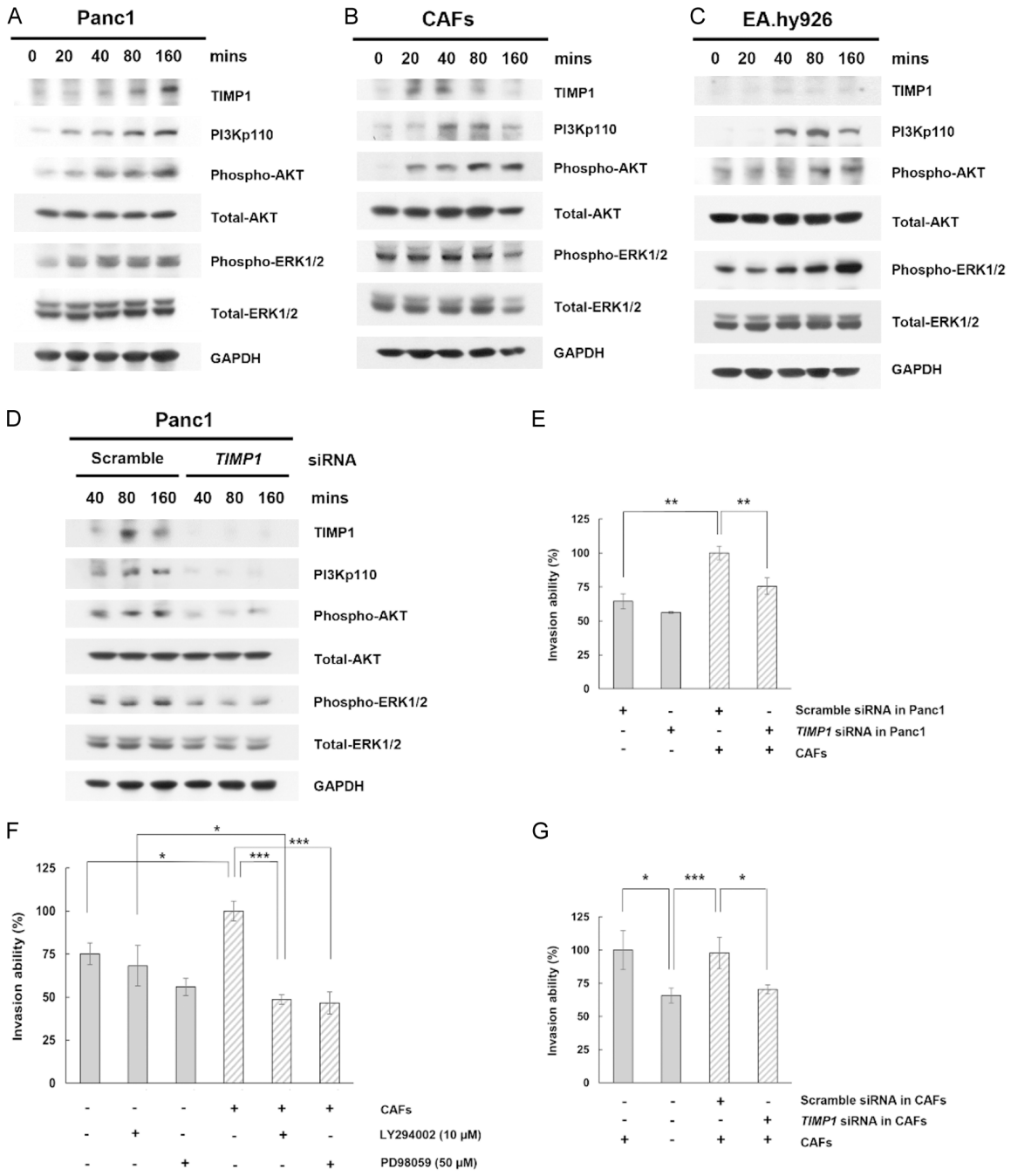

Figure 5. TIMP1-induced invasion ability and related pathways in cell lines under conditions mimicking venous invasion of PDACs. (A-D) Western blot analysis for the expression of TIMP1 and its related proteins (PI3Kp110, phospho-AKT, total-AKT, phospho-ERK1/2, and total-ERK1/2) in each cell line through indirect co-culture of (A) Panc1, (B) CAFs, and (C) EA.hy926 cells at the indicated time points. (D) TIMP1 suppression in Panc1 cells co-cultured indirectly with CAFs and EA.hy926 cells at the indicated times. GAPDH was utilized as the loading control. (E-G) Assessment of invasion ability using endothelial cells coated in the Boyden chamber system. (E) Panc1 or (G) CAFs transfected with TIMP1 or scramble siRNA were allowed to penetrate the matrix and endothelial layer with or without CAFs for 24 hours. (F) The effects of TIMP1 pathway inhibitors (PI3K inhibitor LY294002 at 10 μM or ERK1/2 inhibitor PD98059 at 50 μM) with or without CAFs for 24 hours on Panc1 invasion capability. *P<.05, **P<.01, ***P<.001.

with CD63-positive hepatic stellate cells in circulation, facilitating liver metastasis by creating metastatic niches in mouse models [55]. TIMP1 knockdown in mice and cell lines has

shown a decrease in migration, vascular density, and liver metastasis in PDAC [56, 57], indicating the importance of TIMP1 in the process of distant metastasis in PDAC.

In this study, we focused on identifying the molecules and pathways that contribute to venous invasion as initial steps of metastasis in PDAC, rather than in metastatic sites, and investigated the role of TIMP1 in human PDAC tissues and pancreatic cancer-derived cell lines. Therefore, our study provides more specific and spatially limited information on intravasation and expands our understanding of the role of TIMP1 in the venous invasion of PDAC.

TIMP1 regulates the PI3K/AKT and MAPK/ERK pathways in different types of cancers, including lung [25, 58-61] and colon cancer [25, 58-61], PDAC [25, 58-61], and osteosarcomas [25, 58-61]. In the present study, TIMP1 expression increased concurrently with PI3Kp110, phospho-AKT, and phospho-ERK1/2 in Panc1 cells. TIMP1 knockdown repressed PI3K/AKT and ERK1/2 phosphorylation and decreased Panc1 cell invasion. Moreover, treatment with a PI3K/AKT or ERK1/2 inhibitor suppressed TIMP1-induced invasion. These results suggest that TIMP1 in cancer cells promotes the venous invasion of PDACs by activating the PI3K/AKT and ERK1/2 signaling pathways. Additionally, considering that TIMP1-induced PI3K/AKT or ERK1/2 activation regulates EMT-related transcription factors, such as *TWIST*, *SNAIL*, *SLUG*, and *ZEB1/2* [60, 62], suggests that EMT processes may partially participate in the venous invasion of PDAC cells.

CAFs are a major component of the extracellular matrix (ECM) in PDAC and promote cancer growth through molecular interaction with cancer cells [63-66]. TIMP1 is secreted by CAFs and enhances cancer cell motility and invasion [24, 67, 68]. In the 3D reconstruction of venous invasion foci in PDAC tissues, TIMP1 protein was expressed in cancer cells that participate in damaging the venous wall and the surrounding CAFs. Additionally, the enhancement of CAFs increased their ability to penetrate the endothelial layer of Panc1 cells, while TIMP1 knockdown in CAFs reduced this ability to levels observed in the absence of CAFs. The results of this study suggest that TIMP1 in CAFs plays a crucial role in the venous invasion of PDAC cells induced by CAFs. Previous studies demonstrated that TIMP1 in CAFs stimulates their proliferation through the PI3K/AKT pathway, rather than the ERK1/2 pathway [69], and TIMP1-overexpressing cancer cells promote the accumulation of CAFs [70]. Under co-culture conditions mimicking venous invasion, our data showed the activation of the PI3K/AKT pathway, but not the ERK1/2, in CAFs and an increase of TIMP1 in Panc1 cells. Taken together, we propose that a feedback loop involving the activation of the TIMP1 pathway between CAFs and PDAC cells contributes to the establishment of the tumor microenvironment, facilitating venous invasion in PDACs.

In EA.hy926 cells, the PI3K/AKT and ERK1/2 pathways were activated independently of TIMP1 under co-culture conditions. The ERK1/2 pathway can diminish vascular endothelial junctional proteins, leading to instability in the endothelial barrier [71, 72]. The PI3K/AKT and MAPK/ERK1/2 pathways in human umbilical vein endothelial cells (HUVECs) are associated with changes in mesenchymal-like morphology, increased cell proliferation, angiogenesis, and cancer-associated endothelial cell migration [73, 74]. Therefore, the stimulation of the PI3K/AKT and ERK1/2 pathways in endothelial cells may facilitate cancer cell permeability to veins, representing a crucial step in intravasation. Components of the tumor microenvironment, including PDACs, CAFs, and endothelial cells, interact through TIMP1-related molecular crosstalk to promote the venous invasion of PDACs. Based on our observations and the findings of previous studies, the proposed process of venous invasion in PDAC is illustrated in **Figure 6**.

The results of this study demonstrated the clinical usefulness of TIMP1 as a venous invasion biomarker for PDACs. In the invasion assays, TIMP1 inhibition did not substantially decrease invasion. This result suggests that other factors, aside from TIMP1 expression, contribute to the venous invasion of PDACs. Considering that the microenvironment of PDAC tissues exhibiting venous invasion comprises various cell types - including cancer cells, CAFs, inflammatory cells, venous endothelial cells, and smooth muscle cells - further research utilizing spatial transcriptome analysis is necessary to identify cell-type-specific biomarkers of venous invasion in PDACs. Additionally, a limitation of our functional study is that a single cell

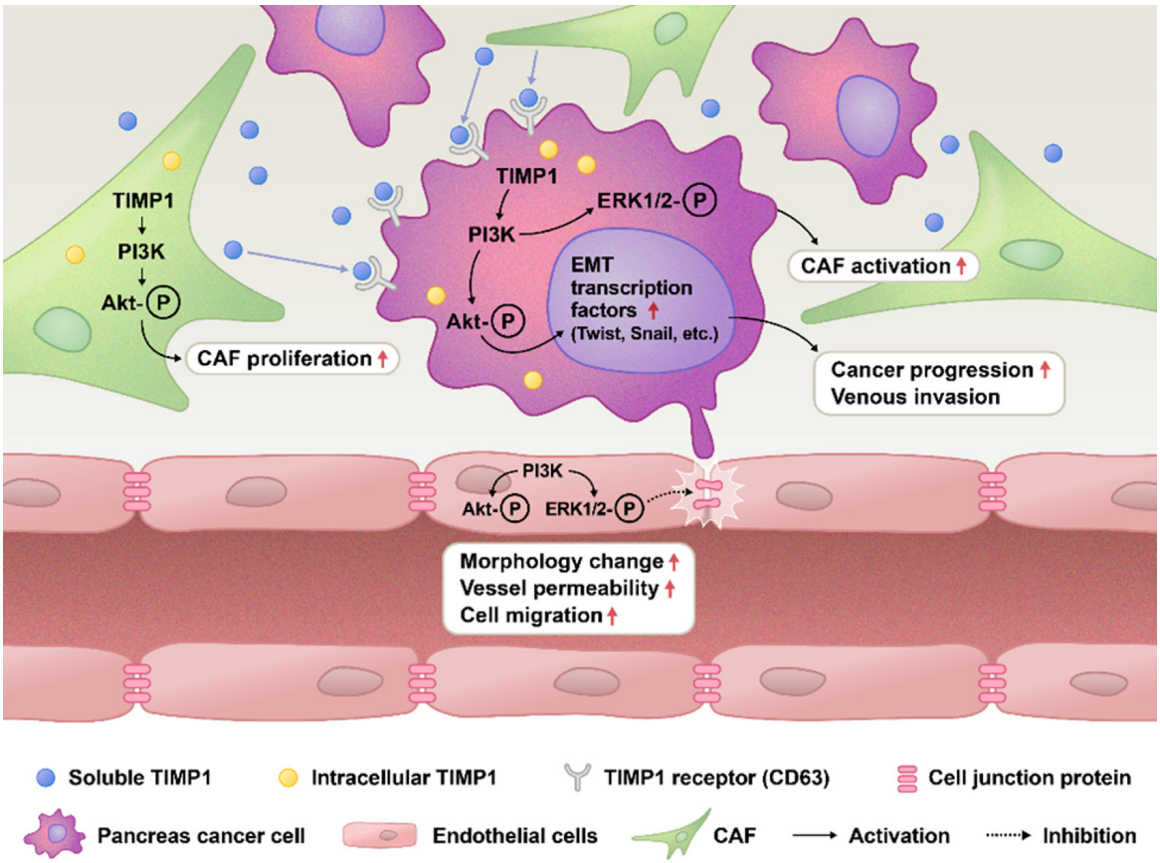

Figure 6. Illustration of TIMP1-induced venous invasion in PDAC. TIMP1 secreted by CAFs stimulates adjacent pancreatic cancer cells. In stimulated cancer cells, activation of EMT-related genes through the TIMP/PI3K/AKT enhances venous invasion, and TIMP1 signaling pathways promote CAFs activation. CAFs and endothelial cells facilitate venous invasion by promoting CAF activation and increasing vascular permeability via the PI3K/Akt and ERK1/2 signaling pathway.

line was employed to represent each component of the tumour microenvironment; therefore, the heterogeneity of PDACs was not fully captured.

CXCR4, identified as a potential gene associated with venous wall invasion through gene expression analysis, is recognized as a hallmark of cancer in various types, including PDACs [75, 76]. Wang *et al*. reported that CXCR4 protein expression is associated with lymph node metastasis and poor survival in patients with PDACs [77]. By contrast, another study assessed CXCR4 expression in PDAC stroma and observed no clinical correlations other than poor differentiation [27]. In this study, the PDAC tissues with venous invasion showed higher nuclear CXCR4 expression than those without venous invasion. However, no other significant differences were observed among other clinicopathologic factors.

In conclusion, TIMP1 was identified as a potential biomarker for venous invasion in PDACs. Furthermore, our results suggest that TIMP1 derived from CAFs activates PDAC cells, promoting venous invasion through the TIMP1/PI3K/AKT and ERK1/2 signaling pathways. The TIMP1 signaling pathway may serve as a potential molecular target for preventing venous wall invasion in patients with PDACs.

Acknowledgements

This study was supported by a grant from the National Research Foundation of the Republic of Korea (NRF-2020R1F1A1076034). This work was presented, in part, at the 35th European Congress of Pathology, Dublin, Ireland, in September 2023. The authors thank Professor Ji Kon Ryu, Seoul National University Hospital, Seoul, Republic of Korea for providing the Panc1 cell line.

Disclosure of conflict of interest

None.

Abbreviations

PDAC, Pancreatic ductal adenocarcinoma; TIMP1, tissue inhibitor of metalloproteinase 1; CXCR4, C-X-C motif chemokine receptor 4; OLFML2B, olfactomedin-like 2B; CYP1B1, cytochrome P450 family 1 subfamily B member 1; CAFs, cancer-associated fibroblasts; PV, portal vein; SMV, superior mesenteric vein; H&E, haematoxylin and eosin; 2D, 2-dimensional; 3D, 3-dimensional; PanIN, pancreatic intraepithelial neoplasia; EMT, epithelial-mesenchymal transition; TCGA, the Cancer Genome Atlas Program; FFPE, formalin-fixed, paraffin-embedded; TMA, tissue microarray; IS, immunohistochemical score; SDS-PAGE, sodium dodecyl sulfate-polyacrylamide gel electrophoresis; MMP, matrix metalloproteinase; ECM, extracellular matrix; HUVEC, human umbilical vein endothelial cell; CXCL12, C-X-C motif chemokine ligand12.

Address correspondence to: Dr. Seung-Mo Hong, Department of Pathology, Brain Korea 21 Project, Asan Medical Center, University of Ulsan College of Medicine, 88, Olympic-ro 43-gil, Songpa-gu, Seoul 05505, Republic of Korea. Tel: +82-2-3010-4558; Fax: +82-2-472-7898; E-mail: smhong28@gmail.com

References

[1] Kang MJ, Jung KW, Bang SH, Choi SH, Park EH, Yun EH, Kim HJ, Kong HJ, Im JS and Seo HG; Community of Population-Based Regional Cancer Registries*. Cancer statistics in Korea: incidence, mortality, survival, and prevalence in 2020. Cancer Res Treat 2023; 55: 385-399.

[2] Jung KW, Kang MJ, Park EH, Yun EH, Kim HJ, Kong HJ, Im JS and Seo HG. Prediction of cancer incidence and mortality in Korea, 2023. Cancer Res Treat 2023; 55: 400-407.

[3] Siegel RL, Miller KD, Wagle NS and Jemal A. Cancer statistics, 2023. CA Cancer J Clin 2023; 73: 17-48.

[4] Sohn TA, Yeo CJ, Cameron JL, Koniaris L, Kaushal S, Abrams RA, Sauter PK, Coleman J, Hruban RH and Lillemoe KD. Resected adenocarcinoma of the pancreas-616 patients: results, outcomes, and prognostic indicators. J Gastrointest Surg 2000; 4: 567-579.

[5] Schnelldorfer T, Ware AL, Sarr MG, Smyrk TC, Zhang L, Qin R, Gullerud RE, Donohue JH, Nagorney DM and Farnell MB. Long-term survival after pancreatoduodenectomy for pancreatic adenocarcinoma: is cure possible? Ann Surg 2008; 247: 456-462.

[6] House MG, Gonen M, Jarnagin WR, D'Angelica M, DeMatteo RP, Fong Y, Brennan MF and Allen PJ. Prognostic significance of pathologic nodal status in patients with resected pancreatic cancer. J Gastrointest Surg 2007; 11: 1549-1555.

[7] Lim JE, Chien MW and Earle CC. Prognostic factors following curative resection for pancreatic adenocarcinoma: a population-based, linked database analysis of 396 patients. Ann Surg 2003; 237: 74-85.

[8] Nakao A, Harada A, Nonami T, Kaneko T and Takagi H. Clinical significance of carcinoma invasion of the extrapancreatic nerve plexus in pancreatic cancer. Pancreas 1996; 12: 357-361.

[9] Strobel O, Hank T, Hinz U, Bergmann F, Schneider L, Springfeld C, Jager D, Schirmacher P, Hackert T and Buchler MW. Pancreatic cancer surgery: the new R-status counts. Ann Surg 2017; 265: 565-573.

[10] Wang J, Lyu SC, Zhou L, Wang H, Pan F, Jiang T, Lang R and He Q. Prognostic analysis of pancreatic carcinoma with portal system invasion following curative resection. Gland Surg 2021; 10: 35-49.

[11] Fukuda S, Oussoultzoglou E, Bachellier P, Rosso E, Nakano H, Audet M and Jaeck D. Significance of the depth of portal vein wall invasion after curative resection for pancreatic adenocarcinoma. Arch Surg 2007; 142: 172-179; discussion 180.

[12] Wang J, Estrella JS, Peng L, Rashid A, Varadhachary GR, Wang H, Lee JE, Pisters PW, Vauthey JN, Katz MH, Gomez HF, Evans DB, Abbruzzese JL, Fleming JB and Wang H. Histologic tumor involvement of superior mesenteric vein/portal vein predicts poor prognosis in patients with stage II pancreatic adenocarcinoma treated with neoadjuvant chemoradiation. Cancer 2012; 118: 3801-3811.

[13] Hruban RH, Gaida MM, Thompson E, Hong SM, Noe M, Brosens LA, Jongepier M, Offerhaus GJA and Wood LD. Why is pancreatic cancer so deadly? The pathologist's view. J Pathol 2019; 248: 131-141.

[14] Smith C, Zheng W, Dong J, Wang Y, Lai J, Liu X and Yin F. Tumor microenvironment in pancreatic ductal adenocarcinoma: implications in immunotherapy. World J Gastroenterol 2022; 28: 3297-3313.

[15] Luo W, Wen T and Qu X. Tumor immune microenvironment-based therapies in pancreatic ductal adenocarcinoma: time to update the concept. J Exp Clin Cancer Res 2024; 43: 8.

[16] Hartupee C, Nagalo BM, Chabu CY, Tesfay MZ, Coleman-Barnett J, West JT and Moaven O. Pancreatic cancer tumor microenvironment is a major therapeutic barrier and target. Front Immunol 2024; 15: 1287459.
[17] Hong SM, Jung D, Kiemen A, Gaida MM, Yoshizawa T, Braxton AM, Noe M, Lionheart G, Oshima K, Thompson ED, Burkhart R, Wu PH, Wirtz D, Hruban RH and Wood LD. Three-dimensional visualization of cleared human pancreas cancer reveals that sustained epithelial-to-mesenchymal transition is not required for venous invasion. Mod Pathol 2020; 33: 639-647.
[18] Krishnan MS, Rajan Kd A, Park J, Arjunan V, Garcia Marques FJ, Bermudez A, Girvan OA, Hoang NS, Yin J, Nguyen MH, Kothary N, Pitteri S, Felsher DW and Dhanasekaran R. Genomic analysis of vascular invasion in HCC reveals molecular drivers and predictive biomarkers. Hepatology 2021; 73: 2342-2360.
[19] Zhang R, Ye J, Huang H and Du X. Mining featured biomarkers associated with vascular invasion in HCC by bioinformatics analysis with TCGA RNA sequencing data. Biomed Pharmacother 2019; 118: 109274.
[20] Mannelqvist M, Stefansson IM, Bredholt G, Hellem Bo T, Oyan AM, Jonassen I, Kalland KH, Salvesen HB and Akslen LA. Gene expression patterns related to vascular invasion and aggressive features in endometrial cancer. Am J Pathol 2011; 178: 861-871.
[21] Zhang L, Wang Z, Li M, Sun P, Bai T, Wang W, Bai H, Gou J and Wang Z. HCG18 participates in vascular invasion of hepatocellular carcinoma by regulating macrophages and tumor stem cells. Front Cell Dev Biol 2021; 9: 707073.
[22] Aljohani AI, Toss MS, Green AR and Rakha EA. The clinical significance of cyclin B1 (CCNB1) in invasive breast cancer with emphasis on its contribution to lymphovascular invasion development. Breast Cancer Res Treat 2023; 198: 423-435.
[23] Jung D, Shin J, Park J, Shin J, Sung YN, Kim Y, Yoo S, Lee BW, Jang SW, Park IJ, Wood LD, Pack CG, Hruban RH and Hong SM. Frequent intraluminal growth of large muscular veins in surgically resected colorectal cancer tissues: a 3-dimensional pathologic reconstruction study. Mod Pathol 2023; 36: 100082.
[24] Song T, Dou C, Jia Y, Tu K and Zheng X. TIMP-1 activated carcinoma-associated fibroblasts inhibit tumor apoptosis by activating SDF1/CXCR4 signaling in hepatocellular carcinoma. Oncotarget 2015; 6: 12061-12079.
[25] Song G, Xu S, Zhang H, Wang Y, Xiao C, Jiang T, Wu L, Zhang T, Sun X, Zhong L, Zhou C, Wang Z, Peng Z, Chen J and Wang X. TIMP1 is a prognostic marker for the progression and metastasis of colon cancer through FAK-PI3K/AKT and MAPK pathway. J Exp Clin Cancer Res 2016; 35: 148.
[26] Shou Y, Liu Y, Xu J, Liu J, Xu T, Tong J, Liu L, Hou Y, Liu D, Yang H, Cheng G and Zhang X. TIMP1 indicates poor prognosis of renal cell carcinoma and accelerates tumorigenesis via EMT signaling pathway. Front Genet 2022; 13: 648134.
[27] Bodoque-Villar R, Padilla-Valverde D, Gonzalez-Lopez LM, Munoz-Rodriguez JR, Arias-Pardilla J, Villar-Rodriguez C, Gomez-Romero FJ, Verdugo-Moreno G, Redondo-Calvo FJ and Serrano-Oviedo L. The importance of CXCR4 expression in tumor stroma as a potential biomarker in pancreatic cancer. World J Surg Oncol 2023; 21: 287.
[28] Na IK, Scheibenbogen C, Adam C, Stroux A, Ghadjar P, Thiel E, Keilholz U and Coupland SE. Nuclear expression of CXCR4 in tumor cells of non-small cell lung cancer is correlated with lymph node metastasis. Hum Pathol 2008; 39: 1751-1755.
[29] Wang P, Yang X, Zhou N, Wang J, Li Y, Liu Y, Xu X and Wei W. Identifying a potential key gene, TIMP1, associated with liver metastases of uveal melanoma by weight gene co-expression network analysis. Onco Targets Ther 2020; 13: 11923-11934.
[30] Huang R, Wang K, Gao L and Gao W. TIMP1 is a potential key gene associated with the pathogenesis and prognosis of ulcerative colitis-associated colorectal cancer. Onco Targets Ther 2019; 12: 8895-8904.
[31] Wurtz SO, Schrohl AS, Mouridsen H and Brunner N. TIMP-1 as a tumor marker in breast cancer--an update. Acta Oncol 2008; 47: 580-590.
[32] Schrohl AS, Holten-Andersen MN, Peters HA, Look MP, Meijer-van Gelder ME, Klijn JG, Brunner N and Foekens JA. Tumor tissue levels of tissue inhibitor of metalloproteinase-1 as a prognostic marker in primary breast cancer. Clin Cancer Res 2004; 10: 2289-2298.
[33] Nakopoulou L, Giannopoulou I, Stefanaki K, Panayotopoulou E, Tsirmpa I, Alexandrou P, Mavrommatis J, Katsarou S and Davaris P. Enhanced mRNA expression of tissue inhibitor of metalloproteinase-1 (TIMP-1) in breast carcinomas is correlated with adverse prognosis. J Pathol 2002; 197: 307-313.
[34] Lee JH, Choi JW and Kim YS. Plasma or serum TIMP-1 is a predictor of survival outcomes in colorectal cancer: a meta-analysis. J Gastrointestin Liver Dis 2011; 20: 287-291.
[35] Wang YY, Li L, Zhao ZS and Wang HJ. Clinical utility of measuring expression levels of KAP1,

TIMP1 and STC2 in peripheral blood of patients with gastric cancer. World J Surg Oncol 2013; 11: 81.
[36] Liu H, Xiang Y, Zong QB, Zhang XY, Wang ZW, Fang SQ, Zhang TC and Liao XH. miR-6745-TIMP1 axis inhibits cell growth and metastasis in gastric cancer. Aging (Albany NY) 2021; 13: 24402-24416.
[37] Grunnet M, Mau-Sorensen M and Brunner N. Tissue inhibitor of metalloproteinase 1 (TIMP-1) as a biomarker in gastric cancer: a review. Scand J Gastroenterol 2013; 48: 899-905.
[38] Gouyer V, Conti M, Devos P, Zerimech F, Copin MC, Creme E, Wurtz A, Porte H and Huet G. Tissue inhibitor of metalloproteinase 1 is an independent predictor of prognosis in patients with nonsmall cell lung carcinoma who undergo resection with curative intent. Cancer 2005; 103: 1676-1684.
[39] Fong KM, Kida Y, Zimmerman PV and Smith PJ. TIMP1 and adverse prognosis in non-small cell lung cancer. Clin Cancer Res 1996; 2: 1369-1372.
[40] Honkavuori M, Talvensaari-Mattila A, Puistola U, Turpeenniemi-Hujanen T and Santala M. High serum TIMP-1 is associated with adverse prognosis in endometrial carcinoma. Anticancer Res 2008; 28: 2715-2719.
[41] Mroczko B, Lukaszewicz-Zajac M, Wereszczynska-Siemiatkowska U, Groblewska M, Gryko M, Kedra B, Jurkowska G and Szmitkowski M. Clinical significance of the measurements of serum matrix metalloproteinase-9 and its inhibitor (tissue inhibitor of metalloproteinase-1) in patients with pancreatic cancer: metalloproteinase-9 as an independent prognostic factor. Pancreas 2009; 38: 613-618.
[42] Schoeps B, Eckfeld C, Prokopchuk O, Bottcher J, Haussler D, Steiger K, Demir IE, Knolle P, Soehnlein O, Jenne DE, Hermann CD and Kruger A. TIMP1 triggers neutrophil extracellular trap formation in pancreatic cancer. Cancer Res 2021; 81: 3568-3579.
[43] Tian Z, Ou G, Su M, Li R, Pan L, Lin X, Zou J, Chen S, Li Y, Huang K and Chen Y. TIMP1 derived from pancreatic cancer cells stimulates Schwann cells and promotes the occurrence of perineural invasion. Cancer Lett 2022; 546: 215863.
[44] Toricelli M, Melo FHM, Hunger A, Zanatta D, Strauss BE and Jasiulionis MG. Timp1 promotes cell survival by activating the PDK1 signaling pathway in melanoma. Cancers (Basel) 2017; 9: 37.
[45] Wojtowicz-Praga SM, Dickson RB and Hawkins MJ. Matrix metalloproteinase inhibitors. Invest New Drugs 1997; 15: 61-75.
[46] Cruz-Munoz W and Khokha R. The role of tissue inhibitors of metalloproteinases in tumorigenesis and metastasis. Crit Rev Clin Lab Sci 2008; 45: 291-338.
[47] Moore CS and Crocker SJ. An alternate perspective on the roles of TIMPs and MMPs in pathology. Am J Pathol 2012; 180: 12-16.
[48] Jung KK, Liu XW, Chirco R, Fridman R and Kim HR. Identification of CD63 as a tissue inhibitor of metalloproteinase-1 interacting cell surface protein. EMBO J 2006; 25: 3934-3942.
[49] D'Angelo RC, Liu XW, Najy AJ, Jung YS, Won J, Chai KX, Fridman R and Kim HR. TIMP-1 via TWIST1 induces EMT phenotypes in human breast epithelial cells. Mol Cancer Res 2014; 12: 1324-1333.
[50] Justo BL and Jasiulionis MG. Characteristics of TIMP1, CD63, and beta1-integrin and the functional impact of their interaction in cancer. Int J Mol Sci 2021; 22: 9319.
[51] Gonzalez LO, Eiro N, Fraile M, Sanchez R, Andicoechea A, Fernandez-Francos S, Schneider J and Vizoso FJ. Joint tumor Bud-MMP/TIMP count at the invasive front improves the prognostic evaluation of invasive breast carcinoma. Biomedicines 2021; 9: 196.
[52] Seubert B, Grunwald B, Kobuch J, Cui H, Schelter F, Schaten S, Siveke JT, Lim NH, Nagase H, Simonavicius N, Heikenwalder M, Reinheckel T, Sleeman JP, Janssen KP, Knolle PA and Kruger A. Tissue inhibitor of metalloproteinases (TIMP)-1 creates a premetastatic niche in the liver through SDF-1/CXCR4-dependent neutrophil recruitment in mice. Hepatology 2015; 61: 238-248.
[53] Rao VS, Gu Q, Tzschentke S, Lin K, Ganig N, Thepkaysone ML, Wong FC, Polster H, Seifert L, Seifert AM, Buck N, Riediger C, Weisse J, Gutschner T, Michen S, Temme A, Schneider M, Baenke F, Weitz J and Kahlert C. Extravesicular TIMP-1 is a non-invasive independent prognostic marker and potential therapeutic target in colorectal liver metastases. Oncogene 2022; 41: 1809-1820.
[54] Poruk KE, Firpo MA, Scaife CL, Adler DG, Emerson LL, Boucher KM and Mulvihill SJ. Serum osteopontin and tissue inhibitor of metalloproteinase 1 as diagnostic and prognostic biomarkers for pancreatic adenocarcinoma. Pancreas 2013; 42: 193-197.
[55] Grunwald B, Harant V, Schaten S, Fruhschutz M, Spallek R, Hochst B, Stutzer K, Berchtold S, Erkan M, Prokopchuk O, Martignoni M, Esposito I, Heikenwalder M, Gupta A, Siveke J, Saftig P, Knolle P, Wohlleber D and Kruger A. Pancreatic premalignant lesions secrete tissue inhibitor of metalloproteinases-1, which activates hepatic stellate cells via CD63 signaling to create a premetastatic niche in the liver. Gastroenterology 2016; 151: 1011-1024, e1017.

[56] D'Costa Z, Jones K, Azad A, van Stiphout R, Lim SY, Gomes AL, Kinchesh P, Smart SC, Gillies McKenna W, Buffa FM, Sansom OJ, Muschel RJ, O'Neill E and Fokas E. Gemcitabine-Induced TIMP1 attenuates therapy response and promotes tumor growth and liver metastasis in pancreatic cancer. Cancer Res 2017; 77: 5952-5962.
[57] Bloomston M, Shafii A, Zervos E and Rosemurgy AS. TIMP-1 antisense gene transfection attenuates the invasive potential of pancreatic cancer cells in vitro and inhibits tumor growth in vivo. Am J Surg 2005; 189: 675-679.
[58] Zhang J, Wang J, Yue K, Li P, Shen W, Qiao X, Wang Y and Wu X. FAM83B promotes the invasion of primary lung adenocarcinoma via PI3K/AKT/NF-kappaB pathway. BMC Pulm Med 2023; 23: 32.
[59] Wang L, Wang J and Chen L. TIMP1 represses sorafenib-triggered ferroptosis in colorectal cancer cells by activating the PI3K/Akt signaling pathway. Immunopharmacol Immunotoxicol 2023; 45: 419-425.
[60] Tian Z, Tan Y, Lin X, Su M, Pan L, Lin L, Ou G and Chen Y. Arsenic trioxide sensitizes pancreatic cancer cells to gemcitabine through downregulation of the TIMP1/PI3K/AKT/mTOR axis. Transl Res 2023; 255: 66-76.
[61] Su Y, Wan D and Song W. Dryofragin inhibits the migration and invasion of human osteosarcoma U2OS cells by suppressing MMP-2/9 and elevating TIMP-1/2 through PI3K/AKT and p38 MAPK signaling pathways. Anticancer Drugs 2016; 27: 660-668.
[62] Jung YS, Liu XW, Chirco R, Warner RB, Fridman R and Kim HR. TIMP-1 induces an EMT-like phenotypic conversion in MDCK cells independent of its MMP-inhibitory domain. PLoS One 2012; 7: e38773.
[63] Kwa MQ, Herum KM and Brakebusch C. Cancer-associated fibroblasts: how do they contribute to metastasis? Clin Exp Metastasis 2019; 36: 71-86.
[64] Joshi RS, Kanugula SS, Sudhir S, Pereira MP, Jain S and Aghi MK. The role of cancer-associated fibroblasts in tumor progression. Cancers (Basel) 2021; 13: 1399.
[65] Asif PJ, Longobardi C, Hahne M and Medema JP. The role of cancer-associated fibroblasts in cancer invasion and metastasis. Cancers (Basel) 2021; 13: 4720.
[66] Singh S, Singh AP and Mitra R. Cancer-associated fibroblasts: major co-conspirators in tumor development. Cancers (Basel) 2024; 16: 211.
[67] Pape J, Magdeldin T, Stamati K, Nyga A, Loizidou M, Emberton M and Cheema U. Cancer-associated fibroblasts mediate cancer progression and remodel the tumouroid stroma. Br J Cancer 2020; 123: 1178-1190.
[68] Nakai N, Hara M, Takahashi H, Shiga K, Hirokawa T, Maeda Y, Yanagita T, Ando N, Takasu K, Suzuki T, Maeda A, Ogawa R, Matsuo Y and Takiguchi S. Cancer cell-induced tissue inhibitor of metalloproteinase-1 secretion by cancer-associated fibroblasts promotes cancer cell migration. Oncol Rep 2022; 47: 112.
[69] Lu Y, Liu S, Zhang S, Cai G, Jiang H, Su H, Li X, Hong Q, Zhang X and Chen X. Tissue inhibitor of metalloproteinase-1 promotes NIH3T3 fibroblast proliferation by activating p-Akt and cell cycle progression. Mol Cells 2011; 31: 225-230.
[70] Gong Y, Scott E, Lu R, Xu Y, Oh WK and Yu Q. TIMP-1 promotes accumulation of cancer associated fibroblasts and cancer progression. PLoS One 2013; 8: e77366.
[71] Mei XY, Zhang JN, Jia WY, Lu B, Wang MN, Zhang TY and Ji LL. Scutellarin suppresses triple-negative breast cancer metastasis by inhibiting TNFalpha-induced vascular endothelial barrier breakdown. Acta Pharmacol Sin 2022; 43: 2666-2677.
[72] Gunduz D, Troidl C, Tanislav C, Rohrbach S, Hamm C and Aslam M. Role of PI3K/Akt and MEK/ERK signalling in cAMP/Epac-mediated endothelial barrier stabilisation. Front Physiol 2019; 10: 1387.
[73] Peng Z, Pang H, Wu H, Peng X, Tan Q, Lin S and Wei B. CCL2 promotes proliferation, migration and angiogenesis through the MAPK/ERK1/2/MMP9, PI3K/AKT, Wnt/beta-catenin signaling pathways in HUVECs. Exp Ther Med 2022; 25: 77.
[74] Cheng HW, Chen YF, Wong JM, Weng CW, Chen HY, Yu SL, Chen HW, Yuan A and Chen JJ. Cancer cells increase endothelial cell tube formation and survival by activating the PI3K/Akt signalling pathway. J Exp Clin Cancer Res 2017; 36: 27.
[75] Sleightholm RL, Neilsen BK, Li J, Steele MM, Singh RK, Hollingsworth MA and Oupicky D. Emerging roles of the CXCL12/CXCR4 axis in pancreatic cancer progression and therapy. Pharmacol Ther 2017; 179: 158-170.
[76] Hanahan D and Weinberg RA. Hallmarks of cancer: the next generation. Cell 2011; 144: 646-674.
[77] Wang Z, Ma Q, Li P, Sha H, Li X and Xu J. Aberrant expression of CXCR4 and beta-catenin in pancreatic cancer. Anticancer Res 2013; 33: 4103-4110.

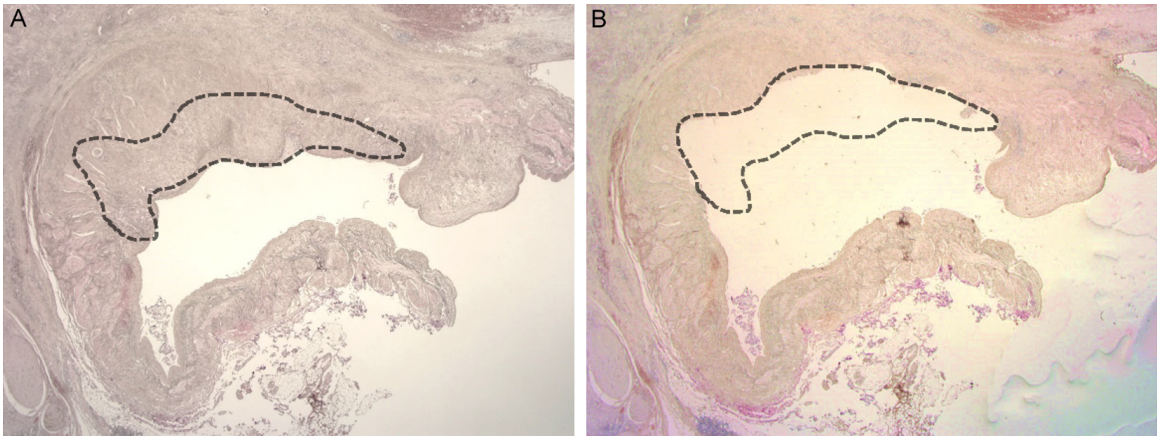

Supplementary Figure 1. Representative images of an uncovered haematoxylin and eosin-stained slide for manual microdissection. The portal vein or superior mesenteric vein with the area of cancer invasion (indicated by dashed lines) before (A) and after (B) manual microdissection.

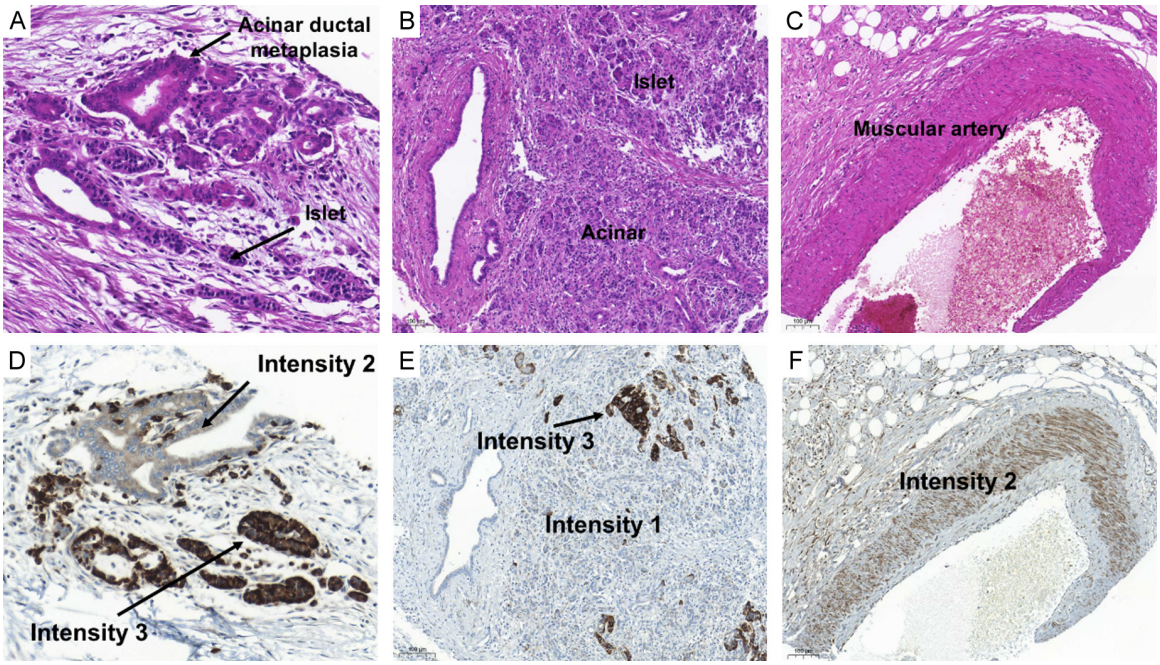

Supplementary Figure 2. Representative images of H&E and TIMP1 immunohistochemical staining of pancreatic tissues, utilized as internal controls for assessing TIMP1 intensity. A-C. H&E images of normal pancreatic islets, acinar cells, acinar ductal metaplasia, and the smooth muscle layer of arteries, which serve as internal controls. D-F. TIMP1 immunohistochemical staining images demonstrating strong intensity (3+) in normal islets, intermediate intensity (2+) in acinar ductal metaplasia and the muscular layer of arteries, and weak intensity (1+) in normal acinar cells.

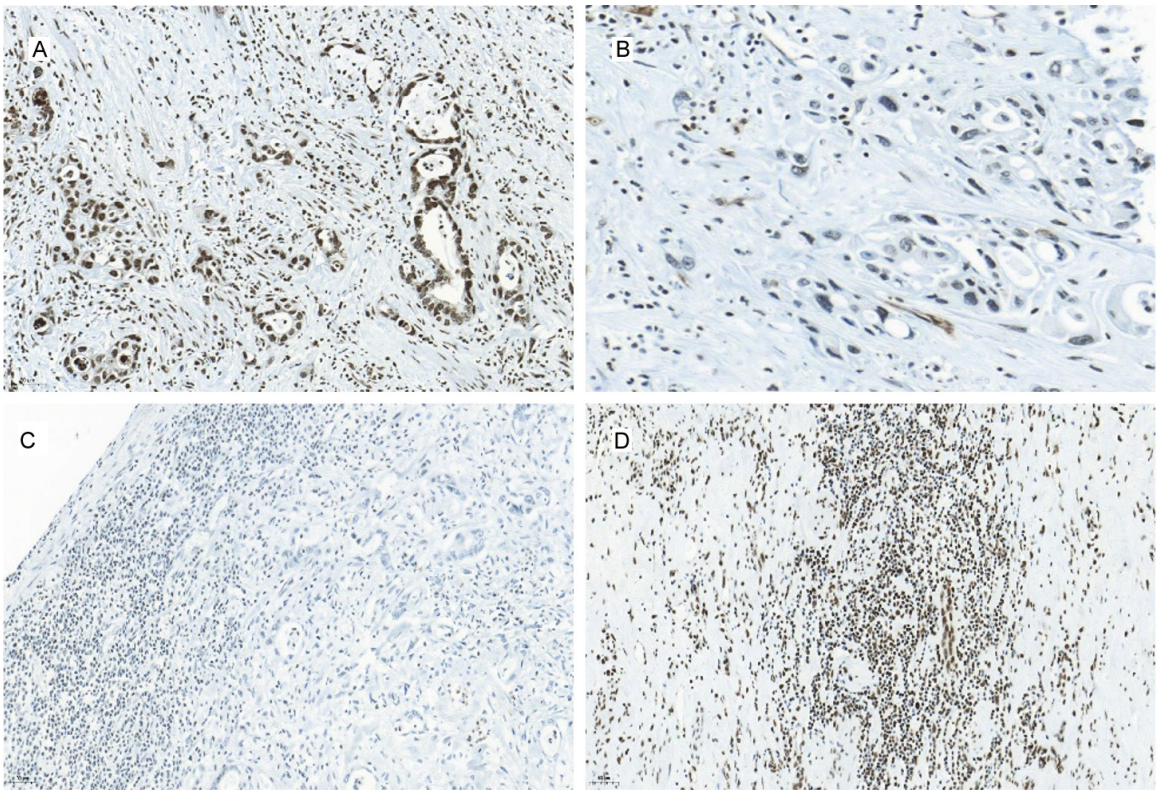

Supplementary Figure 3. Representative CXCR4 immunohistochemical staining images of PDAC tissue with venous invasion with different scores in cancer cells, inflammatory cells, and CAFs. A. Strong nuclear CXCR4 expression (score 2) in cancer cells, inflammatory cells, and CAFs (20×). B. Weak nuclear expression (score 1) in cancer cells (40×). C. No CXCR4 expression (score 0) in cancer cells and CAGs and weak CXCR4 expression (score 1) in inflammatory cells (20×). D. Strong nuclear CXCR4 labelling (score 2) in inflammatory cells (40×).

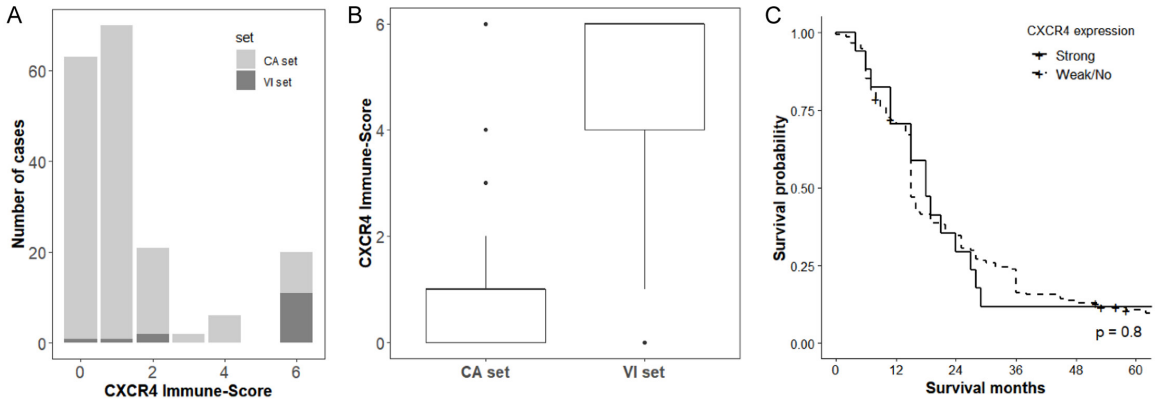

Supplementary Figure 4. Results of CXCR4 immunolabelling in the VI and CA sets. A. The proportion of cases with strong CXCR4 expression (score 6) in the VI set was 55% (11/20), which was higher than that in the CA set (45%, 9/20, P<.001). B. CXCR4 expression in the VI set had a 4.73 ± 2.22 higher immune score than that in the CA set (1.14 ± 1.48, P<.001). C. No significant difference in 5-year overall survival according to CXCR4 expression status (strong CXCR4 expression group, 11.8%; weak/no CXCR4 expression group, 10.6%, P=.8).

Supplementary Table 1. Comparison of CXCR4 expression status with clinicopathologic factors of PDACs

Clinicopathologic factors		CXCR4 expression		*P*-value
		Weak/none	Strong	
Age, years		62.4 ± 9.81	68.59 ± 8.37	.01[a]
Sex	Male	83 (55.3%)	12 (70.6%)	.35
	Female	67 (44.7%)	5 (29.4%)	
Differentiation	Well-differentiated	6 (4.0%)	1 (5.9%)	.85
	Moderately differentiated	120 (80.0%)	14 (82.4%)	
	Poorly differentiated	24 (16.0%)	2 (11.8%)	
Tumour, cm		3.9 ± 1.9	4.4 ± 2.4	.29
Lymphovascular invasion	Present	62 (41.3%)	6 (35.3%)	.83
	Absent	88 (58.7%)	11 (64.7%)	
Perineural invasion	Present	127 (84.7%)	13 (76.5%)	.60
	Absent	23 (15.3%)	4 (23.5%)	
T category	pT1	1 (0.7%)	1 (5.9%)	.14
	pT2	4 (2.7%)	0 (0%)	
	pT3	145 (96.7%)	16 (94.1%)	
N category	pN0	63 (42.0%)	7 (41.2%)	.88
	pN1	67 (44.7%)	7 (41.2%)	
	pN2	20 (13.3%)	3 (17.6%)	

[a]Statistically significant at P<.05.

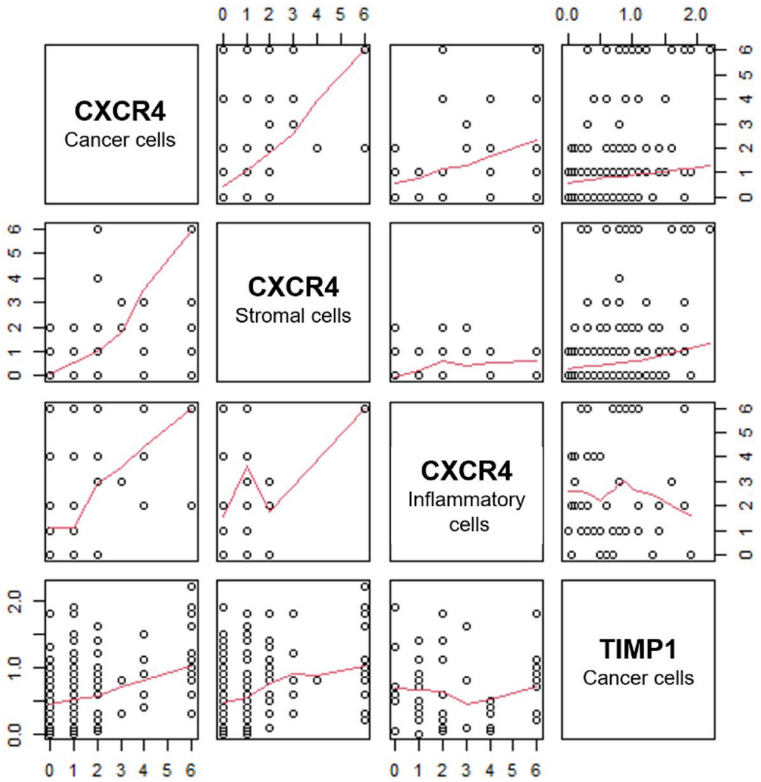

Supplementary Figure 5. Scatter plot showing the association between CXCR4 (Cancer, stromal, and inflammatory cells) and TIMP1 using immunohistochemical score. A correlation was observed between the immunohistochemical scores of CXCR4 cancer, stromal, and inflammatory cells, with correlation coefficients of 0.79, 0.52, and 0.53, respectively. No significant correlation was observed between the immunohistochemical scores of TIMP1 and CXCR4 (cancer, stromal, and inflammatory cells).

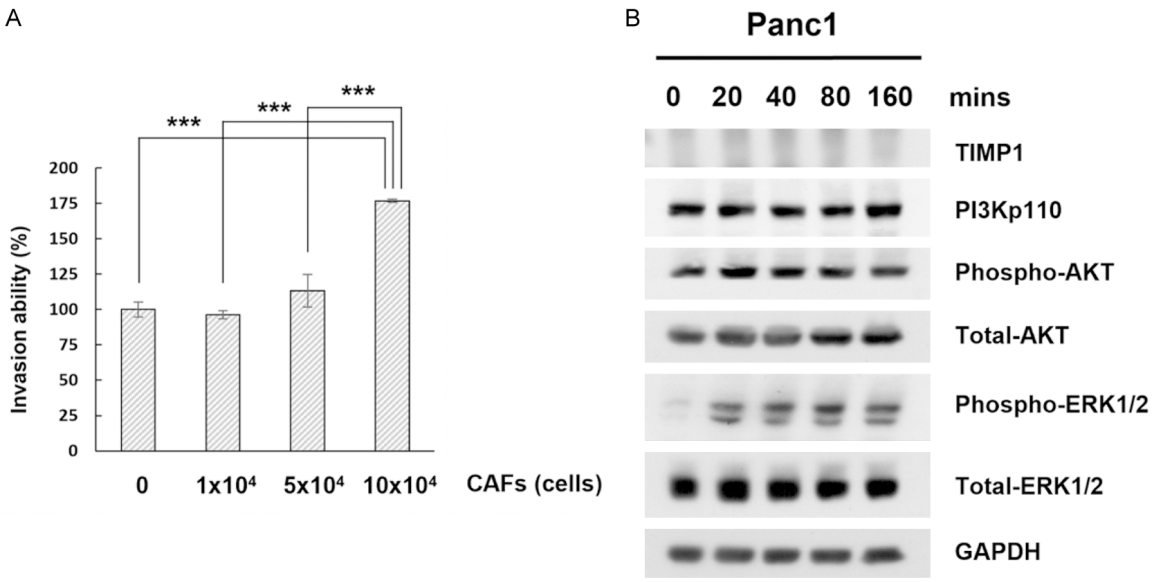

Supplementary Figure 6. Effect of CAFs on venous invasion of PDACs. A. The invasion capability of Panc1 cells was evaluated using endothelial cells in the Boyden chamber system. The invasion of Panc1 cells was assessed with varying quantities of CAFs. An increase in the number of invading Panc1 cells correlated with a higher quantity of CAFs (***P<.001). B. Western blot analysis was conducted to monitor the expression of TIMP1 and its associated proteins, including PI3Kp110, phospho-AKT, total AKT, phospho-ERK1/2, and total ERK1/2 in Panc1 cells through indirect co-culture with EA.hy926 cells at the specified time points. GAPDH was used as the loading control. In the absence of CAFs, Panc1 cells did not induce TIMP1 expression or activate the PI3K/AKT pathway when co-cultured with EA.hy926 cells.